

## Decomposition of $\alpha$ -Aluminum Hydride Power. 2. Photolytic Decomposition

P. J. Herley\* and O. Christofferson

Department of Materials Science and Engineering, State University of New York, Stony Brook, Long Island, New York 11794  
(Received: September 12, 1980; In Final Form: January 28, 1981)

Similarly shaped pressure vs. time curves are obtained in the temperature range from 26 to 70.6 °C from the ultraviolet photolysis of aged  $\alpha$ -AlH<sub>3</sub> powder, pristine and preirradiated with <sup>60</sup>Co  $\gamma$ -rays. The curves consist of an initial deceleratory period followed by a constant rate of gas evolution. The initial-period data can be resolved into one or two exponential terms depending on the sample and/or the pretreatment conditions. At room temperature, increasing the light intensity or preirradiating the material with  $\gamma$ -ray doses greater than  $1.0 \times 10^6$  R increases the rate constants obtained from fitting the kinetic data. Only one exponential term is found below  $1.0 \times 10^6$  R and at high lamp intensities. The linear rate has an almost, but not exact, second-order dependence on the light intensity. The dependence is ascribed to a decomposition event resulting from interaction between two excited radicals, one of which forms a radical-hole pair prior to the interaction. The linear rate deviates further from a second-order dependence for a  $1.0 \times 10^6$  R dose. The activation energies (kJ/mol) of the initial and linear rate periods are 3.2 ( $\pm 0.9$ ) and 13.0 ( $\pm 0.9$ ), respectively. Taken together these results suggest that two processes are initiated by UV light in  $\alpha$ -AlH<sub>3</sub>. The first process involves the interaction of the light-induced carriers with the precursor (intrinsic) defects existing in the material. This process is associated with the lower activation energy. The second process with the larger activation energy is the interaction of the light-induced carriers with each other to produce decomposition in a complex second-order relationship. Both processes are modified by irradiation in a manner consistent with a previously developed phenomenological theory.

### Introduction

This particular aspect of the decomposition of  $\alpha$ -AlH<sub>3</sub> concentrates on the kinetics of the UV-light photolysis. Our earlier investigation<sup>1</sup> indicated that the material could be photolyzed by using high-intensity UV light at room temperature with no significant dark rate. To date the available literature contains no detailed investigation of the photolysis kinetics. However, studies exist<sup>2-5</sup> which do have a direct bearing on the photodecomposition process of polycrystalline AlH<sub>3</sub> at 77 K and at room temperature. For example, EPR signals<sup>2</sup> have been monitored at 77 K and at room temperature after photolysis. Also, the thermostimulated capacitance and dc photoconductivity<sup>3</sup> have been measured together with diffuse optical spectra<sup>4</sup> and low-temperature photoconductivity induced by linearly polarized light.<sup>5</sup>

Collectively these studies indicate that the photoprocess at low temperature produces color centers which are precursors to the development of decomposition nuclei. The color centers create an EPR signal at 77 K and were associated with the presence of two intrinsic crystal defects. These defects were located 3.3-3.4 and 2.4-2.9 eV from the valence band edge. At room temperature these color centers convert rapidly to colloidal aluminum particles which, as the photoprocess proceeds, become "germ" nuclei of metallic aluminum and continue to grow during the decomposition process. It was concluded that the fundamental decomposition step involved the transfer of an electron from an ionization event to the defects in the crystal lattice, thus producing the color centers. This electron transfer process from the Al ion will accordingly

produce H<sup>+</sup> ions (protons) and/or H<sup>-</sup> ions or their respective vacancies which, in turn, diffuse rapidly through the solid at room temperature producing Al metal and H<sub>2</sub> gas. The thermal growth of the colloidal particles into macronuclei was postulated to be dependent on the crystal geometry. Thus, the significant primary step in the photoprocess is one of electron transfer.

However, while these experiments have arrived at conclusions concerning the mobile species and the primary steps of the photodecomposition process, the necessary experimental data are not available to determine the kinetic parameters. Also, if the above-mentioned conclusions are significant, introduction of additional solid-state defects by exposing the material to ionizing radiation, e.g., from  $\gamma$ -rays, should produce significant effects on the subsequent photolysis. Determination of the decomposition kinetics and the effects of  $\gamma$ -irradiation will be the subject of the present investigation. This work has been assisted by a simultaneous scanning electron microscopy (SEM) investigation<sup>6</sup> of the decomposition.

The principles underlying the photoprocesses in solid-state decompositions have been discussed in detail by Jacobs and Tompkins,<sup>7</sup> Young,<sup>8</sup> and Herley and Levy.<sup>9,10</sup> Envisaged as an overall second-order process, i.e., a process involving two chemically distinct entities which may or may not be identical, the primary photo event is assumed to involve solid-state defects normally associated with semiconductor and nonmetal surfaces. These entities include surface (Tamm) states,<sup>11</sup> excitons, electrons, and holes. Development of this phenomenological theory has led to the derivation of an isothermal photolysis equation relating the evolved gas pressure,  $P_1(t)$ , in a closed system

(1) P. J. Herley and R. H. Irwin, *J. Phys. Chem. Solids*, **39**, 1013 (1978).

(2) A. P. Bobrovskii and Yu. D. Pimenov, *Opt. Spectrosc. (Engl. Transl.)*, **39**, 565 (1975).

(3) M. A. Goryaev and Yu. D. Pimenov, *Opt. Spectrosc. (Engl. Transl.)*, **42**, 634 (1977).

(4) Yu. T. Mikhailov, Yu. G. Galitsen, V. V. Boldyrev, and Yu. D. Pimenov, *Opt. Spectrosc. (Engl. Transl.)*, **39**, 651 (1975).

(5) Yu. D. Pimenov, *Opt. Spectrosc. (Engl. Transl.)*, **43**, 53 (1977).

(6) P. J. Herley, O. Christofferson, and J. A. Todd, *J. Solid State Chem.*, **35**, 391 (1980).

(7) P. W. M. Jacobs and F. C. Tompkins, "Chemistry of the Solid State", W. E. Garner, Ed., Butterworths, London, 1955, Chapter 4.

(8) D. A. Young, *Prog. Solid State Chem.*, **5**, 427 (1971).

(9) P. W. Levy and P. J. Herley, *React. Solids, Proc. Int. Symp.*, **6th**, 1968, 75 (1969).

(10) P. W. Levy and P. J. Herley, *Mater. Sci. Res.*, **4**, 156 (1969).

(11) I. Tamm, *Phys. Z. Sowjetunion*, **4**, 733 (1932).

with the time,  $t$ . This equation is of the form

$$P_1(t) = H_1 t - H_2(1 - e^{-h_2 t}) - H_3(1 - e^{-h_3 t}) + H_4(1 - e^{-h_4 t}) \quad (1)$$

where  $h_{2-4}$  and  $H_{1-4}$  are constants associated with the incident light intensity and represent various mechanistic combinations proposed for the rates of formation or destruction of singly excited sites.

An additional result of this theory is an expression relating the steady-state photolytic rate at long times,  $R_1 = (dp/dt)_t$ , to the relative light intensity,  $I/I_0$ :

$$R_1 = \alpha(I/I_0)^2 / [1 \pm \beta(I/I_0)] \quad (2)$$

where  $I_0$  = maximum light intensity and  $\alpha$  and  $\beta$  are constants. When eq 2 has been used, several second-order or very nearly second-order dependencies of the linear rate on relative light intensity have been observed at room temperature.<sup>12-14</sup>

The photochemical decomposition of  $\alpha$ -AlH<sub>3</sub> powder provides a further test for these theories; the solid evolves only hydrogen gas and the process is uncomplicated by complex gas-phase chemical reactions. Also, defects and electronic carriers can be readily introduced into the solid, and these, in turn, should modify the subsequent kinetics if present in sufficient quantity and if they exist for reasonable lifetimes. Temperature effects are important, and these too have been examined, but, for clarity of presentation, data will be presented only for those temperatures at which the thermal dark rate is significantly below the photolytic rate, i.e., between room temperature and 70.6 °C.

## Experimental Section

**Materials.** The material used throughout this entire investigation had aged for a period of 18 months after receipt. Details of the source of the material and its properties are described in part 1. The powder was stored in light-tight containers over anhydrous calcium sulfate (Drierite). All handling procedures were carried out with light excluded wherever possible, and exposure of the samples to air was minimized.

**Apparatus.** Samples (60 mg) distributed over a 0.79-cm<sup>2</sup> area were photolyzed in a conventional Pyrex-glass apparatus similar to an earlier design.<sup>12,14</sup>

The system can also be used to carry out isothermal decomposition studies above room temperature while photolysis is in progress. This function was accomplished by inserting the entire reaction tube into a small furnace. The furnace contained a zirconia-coated copper core with a 1-in.-square hole machined to match the fused-silica optical window. Heating was done with four (6.5 cm (o.d.)  $\times$  10 cm) semicylindrical ceramic heating cores (290 W each), and the furnace temperature was controllable to  $\pm 0.3$  °C.

Ultraviolet (UV) light was produced by a 1000-W, air-cooled, high-pressure mercury lamp (BH6, Illumination Industries, New Jersey) with a broad continuum in the UV region.<sup>12</sup> A 3-in. long water filter inserted in the light path removed the infrared components of the spectrum. The light was focused on the sample by using an achromatic fused-silica lens and a rotatable front-surface plane mirror. The latter feature enabled the light to be focussed either on the sample directly or onto an Eppley thermopile (sensitivity, 0.00813  $\mu$ V  $\mu$ W<sup>-1</sup> cm<sup>-2</sup>) located equidistantly

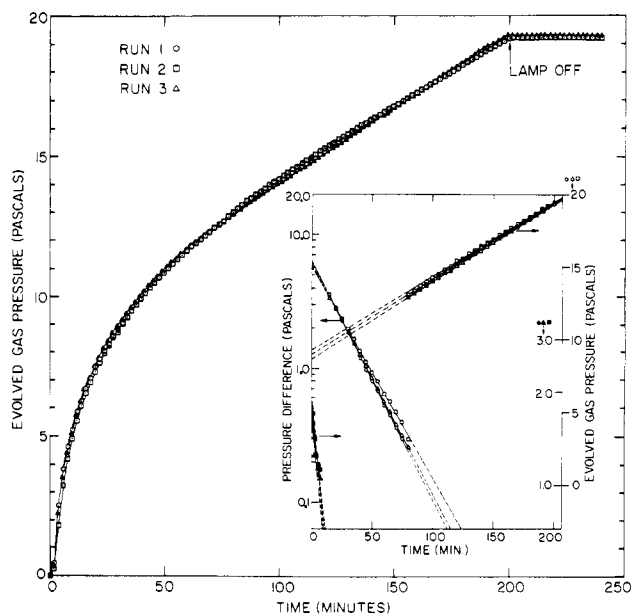


**Figure 1.** Three separate determinations of the gas evolved from 60-mg samples of aluminum hydride powder at room temperature exposed to ultraviolet light from a high-pressure mercury lamp. These data demonstrate the reproducibility obtained. Also shown is the resolution of the data curves into linear and exponential components as described in the text.

from the sample. The lamp intensity was varied by inserting fused-silica, neutral-density filters into the beam path.

**Procedure.** Powders were weighed in air, poured directly into the fused-silica sample holder, leveled, and placed into the system beneath the Supersil window. The sealed system was pumped overnight (12–16 h) at a background pressure of  $\sim 1.2 \times 10^{-7}$  to  $4.0 \times 10^{-7}$  Pa. The outgassing rate of the isolated sample chamber after this period, prior to photolysis, was below 0.001 Pa min<sup>-1</sup>. For a photolysis determination the reaction cell was isolated from the pumps, the background pressure rate was monitored, and, when it had attained a constant rate, the sample was exposed to the light by using a photographic shutter. For runs above room temperature, the furnace was preset and allowed to equilibrate overnight at the desired temperature. The sample boat was not inserted into the illuminated furnace until the experiment commenced.

Pressure data were recovered continuously on a Hewlett Packard strip chart recorder and, after correction for the background rate, were digitized every minute. These data were used for the subsequent mathematical analysis, and all of the data points were included when processed on the UNIVAC 1100 computer. However, the figures in the text show only enough data to delineate the curves.

Samples for  $\gamma$  irradiation were encapsulated in evacuated ( $\sim 10^{-3}$  torr) fused-silica ampules. The ampules were wrapped in aluminum foil to make them light-tight and irradiated at ambient temperatures with <sup>60</sup>Co  $\gamma$ -rays in the spent-fuel facility at Brookhaven National Laboratory. The  $\gamma$ -ray dose rates were  $5.5 \times 10^4$ ,  $1.2 \times 10^6$ , and  $5.3 \times 10^6$  rd h<sup>-1</sup>.

## Results

**Pristine Powder.** The following subsection contains results obtained from a series of experiments designed to probe the photodecomposition of pristine powder.

(i) The pressure ( $P$ ) vs. time curves were reproducible from run to run for a fixed light intensity. A typical series of three consecutive  $P(t)$  curves demonstrating the reproducibility at 26 °C are shown in Figure 1. Gas is

(12) P. J. Herley and D. H. Spencer, *J. Phys. Chem.*, **83**, 1701 (1979).

(13) D. Dougherty and P. J. Herley, submitted to *J. Phys. Chem.*

(14) P. J. Herley and P. W. Levy, *J. Chem. Phys.*, **46**, 627 (1967); **62**, 177 (1975), and the references contained therein.

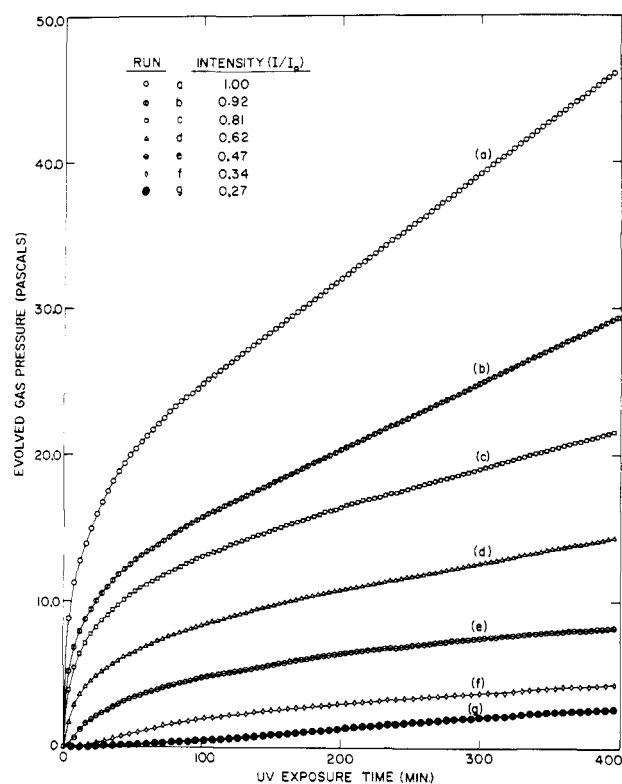


**Figure 2.** Plots of evolved gas vs. time for 60-mg samples of aluminum hydride powder photolyzed at room temperature for relative intensities ( $I/I_0$ ) varying from 1.00 to 0.27.  $I_0$  = maximum intensity = 238 mW  $\text{cm}^{-2}$ .

evolved as soon as the sample is illuminated, and the evolution rate decreases monotonically from the initial maximum and reaches a constant value after  $\sim 100$  min. A dark rate is not discernible at this temperature; i.e., if the light is extinguished at any time during the decomposition, the rate returns to the background outgassing value of the system virtually instantaneously. If the light is extinguished during the constant rate period for various lengths of time ranging from 0.5 to 8 h and the sample then reilluminated, the rate immediately returns to its original linear value.

(ii) The final rate is unchanged when the evolved gas is removed by pumping continuously during the decomposition. This indicates that a significant back-reaction is not occurring and that the reaction is irreversible. No detectable changes in the curve were observed when mechanical mixtures of the pristine powder and final product (finely divided Al powder) in 2:1 ratios were photolyzed at the same lamp intensity as the pristine powder. Attempts to measure the actinic wavelength proved inconclusive. The light transmitted by the monochromator was not sufficiently intense to induce decomposition rates which were different from the background rate.

(iii) The  $P(t)$  curves were affected markedly by varying the total light intensity. As the relative intensity increased, both the rate and the amount of gas evolved increased. The results for relative light intensities ranging from 0.27 to 1.00 are shown in Figure 2 using 60-mg samples at room temperature. The dependence of the final rate on lamp intensity was explored by using multiple, split-run determinations. These results, which were supplemented by additional results from several full-length decompositions, are shown in Figure 3. Also shown is a nonlinear least-squares<sup>15,16</sup> fit of eq 2 to the data (solid line) which yields

(15) D. W. Marquardt, *J. Soc. Ind. Appl. Math.*, **11**, 431 (1963).

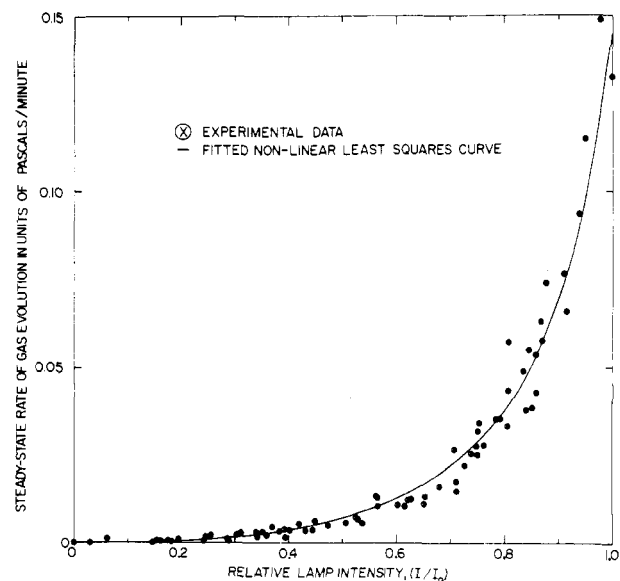


**Figure 3.** Plot of the steady-state photolysis rate vs. relative light intensity for aluminum hydride powder at room temperature. The solid curve is a least-squares fit to the data of  $R_1 = \alpha(I/I_0)^2/[1 - \beta(I/I_0)]$ , where  $\alpha = 0.0174 \pm 0.0016$  Pa  $\text{min}^{-1}$  and  $\beta = 0.886 \pm 0.015$ .  $I_0$  = maximum intensity = 238 mW  $\text{cm}^{-2}$ .

a value of  $0.0174 \pm 0.0016$  Pa  $\text{min}^{-1}$  for  $\alpha$  and  $-0.886 \pm 0.015$  for  $\beta$  when  $I_0$ , the maximum light intensity, is 238 mW  $\text{cm}^{-2}$ .

(iv) Several samples were examined at various stages of the photolysis by using scanning electron microscopy (SEM). After 200-min photolysis the surface layer of the powder possessed a silvery, metallic appearance. The SEM revealed that the photolysis induced the formation of subsurface patches containing fine acicular needles. These needles were identical with the nuclei produced in the thermal decomposition process; the decomposition produced subparticles of acicular needles and was the same in both cases.

(v) Carrying out the photolysis between room temperature and 70.6  $^{\circ}\text{C}$  produced the effects illustrated in Figure 4. At 60  $^{\circ}\text{C}$  and above, a small thermal dark rate was detected slightly above the background value. Any species produced by the photolysis at this temperature will thus have enough thermal energy to continue to decompose slowly after the light is extinguished. Above this temperature simultaneous thermal and photolytic decomposition occurred. This process will be considered in detail in part 3.

(vi) Finally, the room-temperature  $P(t)$  data were analyzed by using the phenomenological kinetic equation<sup>8</sup> (eq 1). This equation fits the data best in the form

$$P = H_1 t - H_2(1 - e^{-h_2 t}) + H_4(1 - e^{-h_4 t}) \quad (3)$$

which suggests that the  $H_3$  term in eq 1 is either inoperable or insignificant in the present case. Thus, the curves are resolvable into two distinct decaying exponentials and into a linear rate (see, for example, the insert in Figure 1 for the three reproducibility runs). All of the constants ( $H_{1,2,4}$ ,  $h_{2,4}$ ) found from fitting this equation to the varying light-intensity data at various temperatures are tabulated in supplementary Tables I and II. (See paragraph at end

(16) D. A. Meeker, nonlinear least-squares program (GAUSHAUS, University of Wisconsin Computing Center, 1964; program revised 1966).

(17) P. J. Herley and D. A. Schaeffer, *J. Phys. Chem.*, **82**, 155 (1978).

(18) J. A. Dilts and E. C. Ashby, *Inorg. Chem.*, **11**, 1230 (1972).

(19) M. A. Gorgaeva and Yu. D. Pimenov, *Sov. J. Opt. Technol. (Engl. Transl.)*, **42**, 538 (1975).

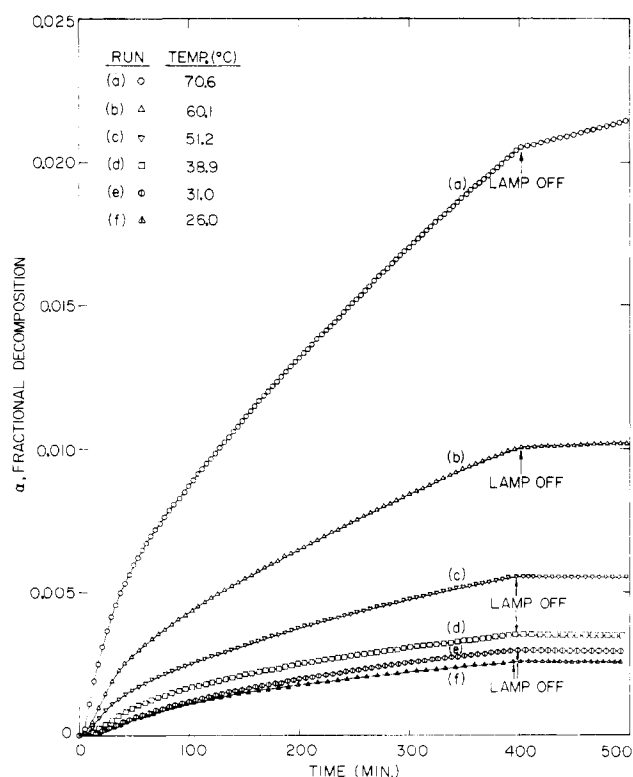


**Figure 4.** Plots of fractional decomposition,  $\alpha = P(t)/P_i$ , vs. time for the photolysis of 60-mg samples of aluminum hydride powder photolyzed isothermally at 26.0, 31.0, 38.9, 51.2, 60.1, and 70.6 °C ( $P(t)$  corresponds to the pressure at time  $t$ , and  $P_i$  to the pressure at complete decomposition for the reaction  $\text{AlH}_3 \rightarrow \text{Al} + \frac{3}{2}\text{H}_2$ ). The lamp intensity was  $79.4 \text{ mW cm}^{-2}$ . Also shown is the effect of temperature on the dark rate, i.e., the rate of gas evolution upon turning off the light during the constant, steady-state period.

of text regarding supplementary material.) The temperature markedly affected both the linear rate and the total amount of gas evolved.

For activation-energy determinations the  $P(t)$  curves were converted to fractional decomposition ( $\alpha$ ) vs. time curves. To obtain a suitable kinetic parameter to define the entire initial deceleratory period, we assumed that the deceleratory rate constant is proportional to  $1/\tau$ , where  $\tau$  is the time required for the reaction to attain a linear rate. The initial-period rate constant,  $k_4$ , was then obtained from the relationship

$$k_4 = 1/\tau \quad (4)$$

The linear-period rate constant was obtained from a fit of

$$\alpha = k_5 t + c_5 \quad (5)$$

( $k_5$  and  $c_5$  are constants) to the data at long times. The specific rate constants are listed in Table III (supplementary material). The activation energies (kJ/mol) found for the initial and linear rate periods are  $3.2 \pm 0.9$  and  $13.0 \pm 0.9$ , respectively.

**Irradiated Powder.** The kinetic behavior of material after exposure to  $^{60}\text{Co}$   $\gamma$ -rays was determined from a series of samples irradiated with doses ranging from  $1.0 \times 10^3$  R to  $1.0 \times 10^9$  R. Three 60-mg samples, each exposed to a  $1.0 \times 10^6$  R dose, yielded pressure vs. time curves which were virtually superimposable. Also, the irradiated material behaves in a manner identical with that of the pristine solid when exposed to most of the pretreatments described in paragraphs ii-iv. However, there are two noteworthy exceptions. Differences occur in the preirradiated-data curves when either the light intensity or the

preirradiation dose is varied.

Variation in the light intensity influences the entire  $P(t)$  curve for relative light intensities between 0.47 and 1.00. Both the evolved gas and the steady-state rate increase with increasing intensity. This behavior is similar to that of the pristine powder; however, different values for the kinetic parameters are obtained when eq 3 is applied to the data. Values for  $1.0 \times 10^6$  rd preirradiated powder are tabulated in (supplementary material) Table IV over the entire intensity range at room temperature. The parameters which are most sensitive to the light-intensity variation are  $H_2$  and  $h_2$  (which are reflected in the increase in the total quantity of gas evolved) and  $H_1$ , the steady-state rate. The irradiated material has a faster rate at all of the measured intensities.

In order to study the relationship between  $H_1$  and the light intensity in more detail we supplemented the entire-run data listed in Table IV by a series of split-run determinations. The nonlinear least-squares fit to the data resulted in values of  $\alpha = 0.0029 \pm 0.0009 \text{ Pa min}^{-1}$  and  $\beta = -0.909 \pm 0.038$  for a maximum light intensity of  $151 \text{ mW cm}^{-2}$ . Apparently, as a result of the preirradiation, the value of  $\alpha$  has decreased while  $\beta$  has increased very slightly within the experimental error.

Changes in the values of the kinetic parameters also occur when the material is exposed to increased doses of  $\gamma$ -rays. Up to  $1.0 \times 10^6$  rd the  $P(t)$  plots do not differ significantly from the unirradiated data. However, from  $5.0 \times 10^6$  to  $1.0 \times 10^9$  rd the total gas evolved over the entire  $P(t)$  curve increased as the dose increased. It is worth noting that a similar increase in evolved gas was observed at the same doses in the preirradiated isothermal decomposition dose sequence carried out at 130 °C and discussed in part 1. The resulting changes in the overall curves are illustrated in Figure 5. All of the  $P(t)$  data could be fitted to eq 3. The resulting rate constants are tabulated in Table V (supplementary material) for the various doses, and it is noticeable that, above a dose of  $1.0 \times 10^8$  rd, the last exponential term becomes negligible. Also, the steady-state rate,  $H_1$ , is little affected by the radiation over the entire dose range, whereas above  $1.0 \times 10^6$  rd the value of  $h_2$ , the exponential constant, drops rapidly.

Finally, several preirradiated samples were examined by using SEM before and after 350-min photolysis at room temperature. The condition of the  $\gamma$ -ray preirradiated material has been described in part 1. After decomposition the photolyzed material is shiny and metallic. During the photolysis localized patches containing acicular nuclei were observed to form close to the surface and were similar to those found in the early stages of the thermolysis but were noticeably higher in density. At the end of the photolysis the subsurface product has the same filamentary appearance as the thermally decomposed product.

## Discussion

The  $P(t)$  curves generated by the photolysis of pristine and  $\gamma$ -ray preirradiated  $\alpha$ -AlH<sub>3</sub> consist of an initial deceleratory component superimposed on a linear rate component. The initial component can be resolved into two exponential terms for pristine material and into one or two exponential terms for preirradiated material depending on the  $\gamma$ -ray dose. The reaction is reproducible and irreversible; at room temperature the light-generated species either decay extremely rapidly or are comparatively stable. The failure of product admixture to catalyze the reaction is not unambiguous. The mixture was not compacted in order to maintain the comparison with the pristine powder decomposition. Also, it is likely that some form of surface

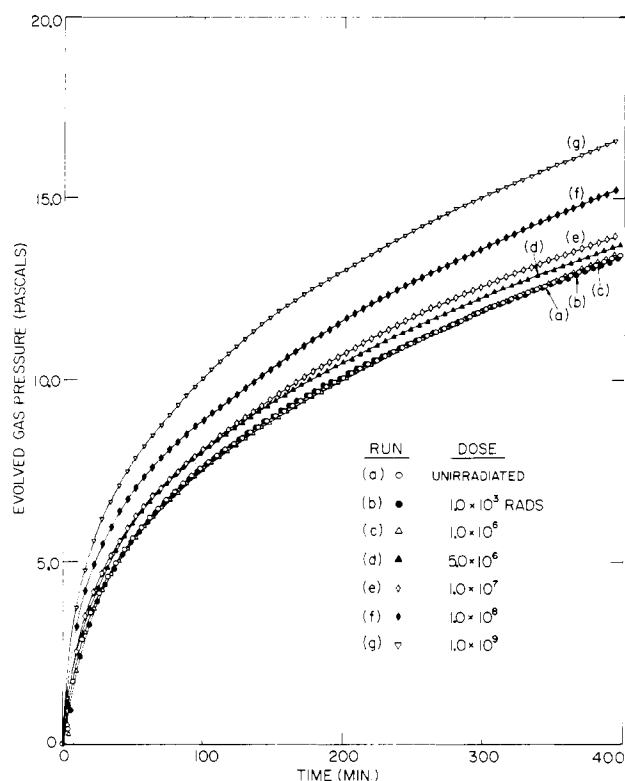


**Figure 5.** Plots of evolved gas pressure vs. time of samples exposed to the indicated  $^{60}\text{Co}$   $\gamma$ -ray doses photolyzed at room temperature. Each 60-mg sample of aluminum hydride powder was photolyzed at a constant lamp intensity of  $122 \text{ mW cm}^{-2}$ . The total  $\gamma$ -ray exposure varied from  $1.0 \times 10^3$  to  $1.0 \times 10^9$  rd. An unirradiated run is included for comparison.

oxide layer will have formed on the product surfaces which impedes catalysis.

The absence of a dark rate at room temperature shows that the light-induced species are not sufficiently thermally activated at this temperature to prolong the decomposition. A relatively small activation energy ( $\sim 3.2 \text{ kJ/mol}$ ) is required to induce a measurable dark rate and provides an explanation for the effect of aging: a combination of above-room-temperature storage and/or prolonged UV exposure will produce decomposition.

It is significant that all of the terms in eq 3 are dependent on the light intensity. These terms include contributions representing a large number of possible physical processes which, in turn, are directly related to the light intensity.<sup>9,10</sup> However, at this time it is not possible to resolve the specific dependence of each process on the light intensity. However, some variations on specific rate constants are evident. For example, the dependence of the steady-state rate on light intensity was modified on exposure to  $\gamma$  irradiation. Although small variations in fitting the equations to the data result in large variations in the values of  $\alpha$  and  $\beta$ , it appears that irradiation has apparently decreased  $\alpha$  while  $\beta$  is only increased slightly. A similar trend was observed in the photolysis of  $\text{NaBrO}_3$  powder.<sup>14</sup> In terms of the proposed theory, an  $\alpha$  increase reflects an increase in the excited-site concentration. If the increase in  $\beta$  is significant, the slight enhancement could be ascribed to the destruction of existing singly excited sites without

forming decomposition product, e.g., by thermal recombination of electron-hole pairs which are presumably enhanced by the presence of the  $\gamma$ -ray-generated defects.

Consideration of the data in Tables IV and V shows that the kinetic analysis yields only one exponential term in the lower  $\gamma$ -ray doses compared to two for the pristine and high-intensity decomposed material. Some indication that the second exponential term is influenced by photon-induced carriers is shown by the fact that two exponential components are found for a  $1.0 \times 10^6$  rd run at low lamp intensity. The radiation effects occurring near  $1.0 \times 10^6$  rd suggest that below this dose the radiation-induced processes which do markedly affect the thermal processes (see part I) produce a minimal effect because of the low density of  $\gamma$ -ray-induced surface sites compared to the photolytically induced surface sites. However, the  $\gamma$ -ray-induced effects can be sufficiently large to remove the smaller of the two exponential terms. Above  $1.0 \times 10^6$  rd, where a color change is also observed, the  $\gamma$ -radiation-induced species are in sufficient numbers on the surface to effect a change during subsequent photolysis. This clearly delineates the bulk vs. surface roles of the two decomposition processes (thermal vs. photolytic). The marked drop in  $h_2$ , the surface precursor rate constant, at a dose of  $1.0 \times 10^6$  rd, reflects this increase in  $\gamma$ -ray-induced defects probably due to the formation of additional traps which decrease the initial rate of gas evolution. In the pristine material exposure to increasing light intensity will increase the carrier concentration, saturate the fixed number of intrinsic traps, and continue on to generate additional decomposition. Thus, the result will be an increase in  $h_2$  with light intensity, as was found experimentally. The observed second-order process can be attributed to the interaction of two identical excited species whose concentration is dependent on the light intensity.

The lower value of the initial-period activation energy results from reaction at the precursor (defect) sites. It is expected that this energy would be lower than the energy of the steady-state uniform penetration of the reaction interface into the bulk material. The activation energies also indicate that two distinct temperature regimes exist. The first is a lower-temperature region in which we propose the purely photolytically induced nucleus formation process occurs. (Decomposition is produced solely by interaction with the UV light.) In the other (high-temperature) regime the activation energy is higher than that of photolysis alone but much lower than that associated with the thermal decomposition. Obviously a synergistic or energetic interaction process is occurring between thermal and photoinduced defects or complexes in this regime.

*Acknowledgment.* This research was supported by the U.S. Department of Energy under Contract No. E(11-1)-2715.

*Supplementary Material Available:* Constants derived from the fit of eq 3 to the photolysis data from pristine and  $\gamma$ -irradiated material are listed in Tables I-V (5 pages). Effects of temperature, light intensity, and  $\gamma$ -ray doses on the constants are included together with listings of the empirical rate constants  $k_4$  and  $k_5$  between 26.0 and 51.2  $^\circ\text{C}$ . Ordering information is given on any current mast-head page.